Internal Report
HERMES 97-021

Analysis of semi-inclusive unpolarized reactions with Λ and $\bar{\Lambda}$ production in HERMES experiment

S.Belostotski, O.Grebenyuk, A.Jgoun, S.Manaenkov, Yu.Naryshkin

July 13, 1997

Contents

1 Introduction

Study of semi-inclusive reactions with $\Lambda(\bar{\Lambda})$ in the final state is of grate interest because Λ is a hyperon polarization of which can be measured through its dominant hadronic decay: $\Lambda \Rightarrow p + \pi^-$ and $\bar{\Lambda} \Rightarrow \bar{p} + \pi^+$.

Importance of measurements of the Λ polarization has been recently pointed out by Jaffe [1]. In current fragmentation region polarization transferred from the polarized lepton to the Λ is sensitive to spin quark distributions in the Λ hyperon and polarization transferred from the longitudinally polarized target to the Λ is sensitive to spin quark distributions in the target nucleon. For the transversely polarized target observation of the Λ polarization would provide first measurements of the transversity distributions.

According to Ellis [2, 3] measuring the polarization of Λ in the target fragmentation region would probe an important hypothesis of the strong spin anticorrelation of $s\bar{s}$ pairs with the target valence quarks. Unfortunately, under present configuration of the HERMES spectrometer measurements in the target fragmentation is practically not feasible. In order to have access to the target fragmentation region the acceptance for low momentum pions from Λ decay must be substantially enlarged. This would be possible in the frame of the Recoil Detector project developed recently [4].

Here we report on investigation of unpolarized semi-inclusive reaction under discussion. Note that for comprehensive analysis of the polarization the unpolarized distributions must be well understood. Investigation of the polarization observables is then assumed to be the next step.

2 Event selection and summary of the experimental results

We selected the events with at least three reconstructed tracks under condition that only one of them is identified as positron. It is implied that for the selected events tracks of the scattered positron coming out of the primary positron vertex and the two hadrons emitted from the secondary Λ decay vertex are reconstructed and the momenta of all particles are measured with the HERMES spectrometer. Standard particle identification (PID) has been used for positrons. A particle is assumed to be the hadron if it does not satisfy to the positron PID. For a hadron pair with hadrons of the opposite charges invariant mass has been calculated. Events corresponding to Λ and $\bar{\Lambda}$ were distinguished by the fact that in laboratory frame momentum of the $p(\bar{p})$ emitted from $\Lambda(\bar{\Lambda})$ vertex is always higher that that of $\pi^-(\pi^+)$.

In order to suppress the combinatorial background the following cuts have been applied:

- Direction of Λ momentum vector $\vec{P}_\Lambda$ should be close to the vector $\vec{v}$ defined by the primary(positron) and secondary (Λ decay) vertices:

$$x_{vp} = \frac{(\vec{v}, \vec{P}_\Lambda)}{|\vec{v}| \cdot |\vec{P}_\Lambda|} > 0.99995.$$

- Minimal distance d_2 between two hadron tracks combined in vertex should be within 1.5 cm

- To separate Λ vertex from positron vertex, lifetime ($c\tau$) of Λ in its rest frame is set to be $3 < c\tau$ cm.We have also restricted very large lifetime by $c\tau < 27$ cm.

Resulting invariant mass distributions for Λ and $\bar{\Lambda}$ with the above cuts obtained using only 1996 year data set are shown in Fig.1. For Λ events experimentally found peak position is 1.1157 GeV, the reference value from Particle Data Group being 1.11568 GeV. In Fig.2 x_F distributions are shown for Λ events found using 1995 and 1996 year data sets with somewhat different cuts($x_{vp} > 0.9995$, $d_2 < 1.5$ cm, $c\tau > 2$ cm for 1995 year data and $x_{vp} > 0.999$, $c\tau > 3$ cm for 1996 year data). One can see that x_F distribution for 1995 year is shifted to higher x_F. This apparatus effect is resulted from dominating in 1995 year "long track" events, i.e. the events with all three detected particles(the positron and the two hadrons) reconstructed through full tracks in the rear part of the HERMES tracker. In addition to "long track" events, there is a substantial part of "short track" events corresponding to pions coming from Λ decay vertex with relatively low momenta. Many of those pions are deflected by the HERMES spectrometer magnet and do not give full tracks downstream the magnet. Their momenta are reconstructed through tracks in wire chambers (Magnet Chambers) located in the magnet gap. In 1996 year HERMES Magnet Chambers were fully operational (which was not the case for 1995 year) and contribution from the short tracks was essentially higher than that in 1995. In average, the short tracks correspond to Λ-s of lower momenta and x_F respectively. The number of short tracks is shown to be sensitive to the quality of track reconstruction in the front part of the detector. With vertex chamber well operational in 1997 year, it is expected that contribution from the short tracks will be additionally increased by a factor of 1.6. This has been shown with the help of HMC by comparison of the short track reconstructions with Standard Reconstruction and No VC methods of HRC.

3 Comparison of experimental data to HMC simulation

At given energy of the primary positron kinematics of a DIS event is determined by the kinematic variables of the scattered positron (e.g. Q^2 and y) which define the 4-momentum of the virtual photon in the positron scattering plane. In semi-inclusive reaction under consideration

$$e + N \rightarrow e' + \Lambda(\bar{\Lambda}) + X \ , \tag{1}$$

the vector of $\Lambda(\bar{\Lambda})$ momentum is measured in addition to the positron kinematics. As like as in many other cases, it is convenient to consider the Λ kinematics in the virtual photon + target nucleon N rest frame. In this system $\theta^{\Lambda}_{\gamma N}$ is the angle of Λ emission. M_X denotes invariant mass of the system X not detected in the reaction particles.

It should be noted that experimentally measured distributions are in principle sensitive to the Λ polarization through the spectrometer acceptance function. In order to estimate this effect HMC simulations have been done for the unpolarized target and two (positive and negative) beam polarization states. The beam polarizations were chosen to be $P_B = \pm(0.55 \pm 0.06)$ which are realistic numbers for 1995-1996 year running period and polarization transfer from the longitudinally polarized positron to the Λ is assumed to be maximal for both polarization states. The effect of the Λ polarization on the distributions over kinematic variables in question is shown to be negligibly small.

Results of comparison of those distributions to the unpolarized HMC calculations are presented in Figs.3,4 and 5. The 1996 experimental data set (Fig.2) of 3817 Λ events with $Q^2 > 0.8$ (GeV/c)^2 have been used for the comparison. Under identical experimental conditions semi-inclusive Λ events were generated with 3989 HMC Λ events reconstructed. Both the experimental and MC distributions were normalized to unity. One can see that HMC results for kinematic variables related to the scattered positron are in qualitative agreement with the experimental data. Slope parameters for the Q^2 and x_{Bj} distributions are well reproduced by HMC. A noticeable disagreement is found for M_X distribution, the experimental data being apparently shifted to higher M_X. In addition, P_t^2 distribution is less peaked at small P_t^2 compared to HMC predictions.

4 Summary of the Λ yields from 1995 and 1996 year data taking.

It is convenient to scale number of Λ events to the corresponding number of inclusive DIS events. DIS events were selected with the following cuts: $Q^2 > 1.0$ (GeV/c)^2, $W^2 > 4.0$ (GeV)^2, $y < 0.85$ and $0.02 < x_{Bj} < 0.8$ (standard DIS cuts). Due to the fact that the numbers of short tracks were different in 1996 and 1995 years only long track events were taken for comparison. After correction for the calorimeter threshold (which was 3.5 GeV in 1995 and 1.5 GeV in 1996 years, respectively) we arrived at 350 Λ events per 10^6 DIS in 1995 year and 445 Λ events per 10^6 DIS in 1996 year. This discrepancy is practically gone if one applies DIS cuts to the positron associated with Λ production. In Fig.6 Λ yields are shown for hydrogen, deuterium and ^{3}He targets with DIS cuts (lower panel) and without DIS cuts (upper panel). The ^{3}He point is obtained by averaging the 1995 and 1996 data sets. The normalized yields with DIS cuts do not show any target dependence. The behaviour of the yields without DIS cuts is still to be understood. It could be affected by an apparatus effect like sensitivity of number of reconstructed positrons to the calorimeter threshold found to be important if DIS cuts are not applied. It is also not excluded that absorption and rescattering effects are more essential for ^{3}He which perhaps levels down the yields from that target. Unfortunately statistics of 1996 year ^{3}He data is not sufficient to come to final conclusion. In table 1 the yields based on 1996 year data set are summarized for different targets. DIS cuts are applied and short tracks are included. An estimation of the number of normalized Λ events

	^{1}H	^{2}D	^{3}He
N^{Λ} (acc)	1180	1094	421
N^{DIS}, 10^6 (acc)	2.62	2.39	0.75
N^{Λ} /10^6 DIS (acc)	451 $\pm$ 42	458 $\pm$ 44	562 $\pm$ 79
N^{Λ}, 10^4 (4π)	19.77	18.33	7.05
N^{DIS}, 10^6 (4π)	5.94	5.43	1.70
N^{Λ} /10^2 DIS (4π)	3.32 $\pm$ 0.31	3.38 $\pm$ 0.32	4.14 $\pm$ 0.58
$\int dtL$, 10^8	1.54	1.73	0.48
$\frac{\int dtL}{\frac{Z}{A}K}$, $\frac{nucleon}{pb}$	48.66	54.89	15.21

Table 1: Summary of Λ yields,1996 data set

is done for 4π acceptance case. The overall efficiencies to detect both Λ and inclusive DIS events with HERMES spectrometer have been calculated with the help of HMC. They have been found to be $E^{\Lambda} = 0.00597 \pm 0.0002$ and $E^{DIS} = 0.44023$, respectively. An averaged over the targets number of Λ events scaled to 100 inclusive DIS is 3.45 ± 0.21. Note that the latter number is only relevant if DIS cuts are applied. An attempt has been undertaken to specify for each target absolute luminosity numbers (the last line in the table 1). For that integrated within kinematic limits defined by the DIS cuts inclusive DIS cross section for the hydrogen target has been calculated to be $\sigma^{DIS} = 122.17$ nb and counts of LUMI monitor been have normalized with the constant $K = 3.16{\cdot}10^6$ pb/nucleon. The details of absolute normalization and evaluation of DIS cross section can be found in Appendix.

5 Differential cross section of the $e + N \rightarrow e' + \Lambda(\bar{\Lambda}) + X$ reaction.

Similar to the inclusive DIS cross section,the cross section of the semi inclusive Λ production can be written as a function of y and Q^2. With the help of HMC detection efficiencies $\epsilon(Q^2, y)$ of the HERMES spectrometer have been calculated as ratios of reconstructed to generated events in the cells shown in Fig.7. Highly populated by Λ events region at $Q^2 < 1\ (GeV/c)^2$ is excluded because of DIS cuts. The calculations have been done both for semi-inclusive reaction (1) and inclusive DIS and the results are respectively shown in Fig.8 and in Fig.13.

Normalized to unity differential cross section of the reaction was calculated in each cell in Fig.7 as following

$$\frac{1}{\sigma^\Lambda}\frac{d\sigma^\Lambda}{dQ^2dy} = \frac{1}{N^\Lambda}\frac{\Delta N^\Lambda}{\Delta Q^2 \Delta y\ \epsilon(Q^2, y)}, \tag{2}$$

where N^Λ is total number of Λ events for 4π acceptance, obtained as

$$N^\Lambda = \Sigma \frac{\Delta N^\Lambda}{\epsilon(Q^2, y)}$$

with summing up over all the cells in Fig.7, and σ^Λ is corresponding cross section normalization factor for 4π acceptance. It is obvious that $\sigma^\Lambda < \sigma^\Lambda_{tot}$, where the latter is the total cross section of the reaction without any kinematic restrictions.

The numbers of reconstructed by the spectrometer events ΔN^Λ have been obtained from the invariant mass spectra for each cell, the background being subtracted. Due to the fact that scaled to DIS number of Λ events does not depend on the target (see table (1)) all the 1996 year data have been used without distinguishing between the targets. We have obtained for the 1996 year data set

$$N^\Lambda = 23.03 \cdot 10^4$$

with corresponding number of DIS

$$N^{DIS} = 13.07 \cdot 10^6.$$

Normalized to unity cross section points are listed in table 2 and shown in Fig.9 for $1 < Q^2 < 3\ (GeV/c)^2$ and $3 < Q^2 < 5\ (GeV/c)^2$ sets.

In order to evaluate absolute normalization of the reaction cross section given by eq.(2) one has to calculate normalization factor σ^Λ:

$$\sigma^\Lambda = \frac{N^\Lambda}{N^{DIS}}\sigma^{DIS}_{tot}.$$

	$1< Q^2 <3$	$3< Q^2 <5$	$5< Q^2 <7$
	$\langle Q^2\rangle= 1.742$	$\langle Q^2\rangle = 3.776$	$\langle Q^2\rangle = 5.828$
$0.15< y <0.25$	1.49 ± 0.29	-	-
$0.25< y <0.35$	0.72 ± 0.11	-	-
$0.35< y <0.45$	0.71 ± 0.08	0.11 ± 0.02	-
$0.45< y <0.55$	0.45 ± 0.06	0.08 ± 0.02	0.045 ± 0.013
$0.55< y <0.65$	0.44 ± 0.06	0.08 ± 0.02	0.027 ± 0.010
$0.65< y <0.75$	0.35 ± 0.05	0.045 ± 0.016	0.051 ± 0.015
$0.75< y <0.85$	0.31 ± 0.05	0.058 ± 0.023	0.038 ± 0.022

Table 2: Normalized to unity differential cross sections $\frac{1}{\sigma^{\Lambda}}\frac{d^2\sigma(ep\to e'\Lambda X)}{dydQ^2}$ in (GeV/c)$^{-2}$.

Here σ_{tot}^{DIS} is total DIS cross section restricted by DIS cuts. The cross section normalization can be specified for the proton or neutron target nucleon N in (1) by using σ_{tot}^{DIS} for the scattering from the proton and the neutron, respectively. The reaction cross section points for the proton target normalized to σ_{tot}^{DIS} = 122.17 nb (see preceding section and Appendix) are listed in table (3) and shown in Fig.10.

The differential cross section of reaction (1) can be translated to the cross section of the reaction of Λ production by virtual photon as following

$$\frac{d^2\sigma(ep\to e\Lambda X^+)}{dydQ^2} = \Gamma_T\sigma(\gamma^* p\to\Lambda X^+)\ , \tag{3}$$

where Γ_T, the flux of transverse virtual photons, is equal to

$$\Gamma_T = \frac{\alpha(1+(1-y)^2)}{2\pi y Q^2}\ . \tag{4}$$

Obtained in the experiment $\gamma^* p$ cross section can be extrapolated to the point $Q^2 = 0$ to be compared to the SLAC experiment performed at the energy of 20 GeV of the real photon beam[5]. The HERMES data averaged in the range $0.55 < y < 0.85$ along with the SLAC point are shown in Fig.11. The solid line is given by exponent passing through the SLAC experimental point with the slope parameter equal to that experimentally obtained (see Fig.4).

	$1< Q^2 <3$	$3< Q^2 <5$	$5< Q^2 <7$
	$\langle Q^2\rangle = 1.742$	$\langle Q^2\rangle = 3.776$	$\langle Q^2\rangle = 5.828$
$0.15< y <0.25$	2.898 ± 0.566	-	-
$0.25< y <0.35$	1.397 ± 0.215	-	-
$0.35< y <0.45$	1.382 ± 0.160	0.209 ± 0.044	-
$0.45< y <0.55$	0.865 ± 0.107	0.149 ± 0.036	0.087 ± 0.025
$0.55< y <0.65$	0.861 ± 0.110	0.158 ± 0.036	0.052 ± 0.020
$0.65< y <0.75$	0.674 ± 0.091	0.087 ± 0.032	0.099 ± 0.030
$0.75< y <0.85$	0.594 ± 0.093	0.111 ± 0.044	0.074 ± 0.043

Table 3: Absolutely normalized differential cross sections $\frac{d^2\sigma(ep\to e'\Lambda X)}{dydQ^2}$ in nb $(\mathrm{GeV/c})^{-2}$.

Following to the Quark Parton Model (QPM) in unpolarized case one has

$$\frac{d^2\sigma(ep\to e\Lambda X^+)}{dydQ^2} = \frac{2\pi\alpha^2}{Q^4}\Big[1+(1-y)^2) - \frac{Q^2}{2E_e^2}\Big]\Phi^\Lambda(x), \tag{5}$$

where $x = Q^2/(2m_N E_e y)$ is Bjorken scale variable. The semi-inclusive structure function Φ^Λ in eq.(5) reads

$$\Phi^\Lambda(x) = x\sum_q e_q^2 q(x) D_q^\Lambda \ . \tag{6}$$

Here e_q is the fractional electric charge of the quark of a flavour q, sum in (6) runs over all quark flavours, $q(x)$ denotes unpolarized parton distribution in the target. The numbers D_q^Λ are given by

$$D_q^\Lambda = \int_0^1 dz D_q^\Lambda(z)\ , \quad z = \frac{E_\Lambda}{\nu}\ , \tag{7}$$

where $D_q^\Lambda(z)$ is the fragmentation function of a quark q into the Λ. Taking into account eqs.(5,6), we obtain

$$\frac{d^2\sigma(ep\to e\Lambda X^+)}{dydQ^2} = \frac{\pi\alpha^2}{yQ^2 m_p E_e}\Big[1+(1-y)^2) - \frac{Q^2}{2E_e^2}\Big]\sum_q e_q^2 q(x) D_q^\Lambda \ . \tag{8}$$

Finally, neglecting the term $\frac{Q^2}{2E_e^2}$, which is at most equal to 0.032, we obtain

$$\sigma(\gamma^* p \to \Lambda X^+) = \frac{2\pi^2\alpha}{m_p E_e} \sum_q e_q^2 q(x) D_q^\Lambda \ , \tag{9}$$

As it follows from HMC studies[6] Λ production in HERMES experiment is dominated by the struck u quark (about 70% of the Λ yield). We have approximated the cross section given by eq.(9) using dependence $u(x)$ taken from[7]

$$\sum_q e_q^2 q(x) D_q^\Lambda \simeq (4/9) u(x) D_u^\Lambda$$

and treating D_u^Λ as parameter to fit. The result is shown in Fig.12 with $D_q^\Lambda = 0.078$.

A Appendix. DIS differential cross sections

From [8] we have

$$\frac{d^2\sigma(x, Q^2, E)}{dy dQ^2} = \frac{4\pi\alpha^2}{Q^4} \frac{F_2(x, Q^2)}{y} [1 - y - \frac{Q^2}{4E^2} + (1 - \frac{2m_e^2}{Q^2}) \frac{y^2 + Q^2/E^2}{2(1 + R(x, Q^2))}] \ . \tag{10}$$

The nucleon structure function $F_2(x, Q^2)$ is parametrized in [8] as following

$$F_2(x, Q^2) = A(x) \left(\frac{\ln(Q^2/\Lambda^2)}{\ln(Q_0^2/\Lambda^2)} \right)^{B(x)} (1 + \frac{C(x)}{Q^2}) \ , \tag{11}$$

with Q^2 =20 GeV^2, Λ =0.250 GeV and

$$\begin{aligned} A(x) &= x^{a_1}(1-x)^{a_2} \\ &\left[a_3 + a_4(1-x) + a_5(1-x)^2 + a_6(1-x)^3 + a_7(1-x)^4 \right] \ , \\ B(x) &= b_1 + b_2 x + b_3/(x + b_4) \ , \\ C(x) &= c_1 x + c_2 x^2 + c_3 x^3 + c_4 x^4 \end{aligned}$$

The parametrization of the ratio $R = \sigma_L/\sigma_T$ of the longitudinal and transverse cross sections is given by [9]:

$$R(x, Q^2) = \frac{b_1}{\ln(Q^2/\Lambda^2)} \Theta(x, Q^2) + \frac{b_2}{Q^2} + \frac{b_3}{Q^2 + 0.3^2} \ ,$$

where Λ =0.2 GeV and

$$\Theta(x,Q^2) = 1 + 12\ \frac{Q^2}{Q^2+1}\ \frac{0.125^2}{0.125^2+x^2}\ .$$

We have normalized our DIS cross section by the integral

$$\sigma^{DIS} \equiv \int_1^{24} dQ^2 \int_{y_{min}(Q^2)}^{0.85} dy \frac{d^2\sigma(x,Q^2,E)}{dy dQ^2} = 122.17\ \ nb$$

The latter number has been used for absolute normalization both for Λ production and DIS cross sections. The DIS differential efficiencies are shown in Fig.13. The DIS cross sections absolutely normalized are listed in table 4 and shown in Fig.14. The curves are calculated as functions of y using eq.(10). The radiative corrections are important in particular at high y. The experimental data have been multyplied by the radiative correction factor calculated for each y Q^2 bin [10].

We have also undertaken an attempt to find LUMI normalization constant for 1996 year running period proceeding from the above number of σ^{DIS}. For the events selected in 96DST, with our data quality cuts and the same DIS cuts we obtained for the proton target

$$N^{DIS} = 2.617\ 10^6.$$

The experimental total cross section is determined as

$$\sigma^{DIS} = \frac{N^{DIS}}{E^{DIS}\cdot L}\ ,$$

where E^{DIS} is the *overall efficiency of DIS positron* detection in HERMES and L is the integrated luminosity. Monte Carlo simulation gave

$$E^{DIS} = 0.44023\ .$$

Then for the proton target

$$\frac{2.617\cdot 10^6}{0.44023\cdot L} = 122.17\ \rightarrow\ L = 48.66\ \frac{nucleon}{pb}\ .$$

It results in luminosity constant

$$K = 3.16\cdot 10^6\ \frac{pb}{nucleon},$$

to be compared with $K = 2.46\cdot 10^6$ and $K \approx 2.2\cdot 10^6$ given in M.Dueren report[11] and by luminosity group[12] , respectively.

	$1< Q^2 <3$	$3< Q^2 <5$	$5< Q^2 <7$
$0.15< y <0.25$	132.80 ± 1.47	-	-
$0.25< y <0.35$	90.47 ± 0.94	-	-
$0.35< y <0.45$	65.97 ± 0.65	10.95 ± 0.09	-
$0.45< y <0.55$	49.95 ± 0.47	8.75 ± 0.07	3.08 ± 0.02
$0.55< y <0.65$	39.06 ± 0.35	7.24 ± 0.06	2.66 ± 0.02
$0.65< y <0.75$	33.18 ± 0.29	6.24 ± 0.05	2.35 ± 0.02
$0.75< y <0.85$	32.96 ± 0.28	6.07 ± 0.06	2.22 ± 0.04

Table 4: Absolutely normalized inclusive cross sections $\frac{d^2\sigma(ep\to e'X)}{dydQ^2}$ in nb $(\mathrm{GeV/c})^{-2}$.

References

[1] R.L. Jaffe. Polarized Lambdas in the current fragmentation region. *MIT preprint*, Draft notes, 1996.

[2] J. Ellis D. Kharzeev and A. Kotzinian. The proton spin puzzle and Λ polarization in deep-inelastic scattering. *CERN-TH/95-135*, 1995.

[3] J. Ellis D. Kharzeev and A. Kotzinian. *Z. Phys*, C69:467, 1996.

[4] S. Belostotski, M. van Beuzekom, K.Fiedler, O.Grebenyuk, M. G. Guidal, W. H. A. Hesselink, E.Kok, G. van der Steenhoven, J.J.M.Steijger and V.Vikhrov. Internal Report HERMES 97-019

[5] K.Abe et al. Inclusive photoproduction of neutral strange particles at 20 GeV. *Phys. Rev.*, D29:1877, 1984.

[6] S.Belostoski et al. Monte Carlo studies of Λ production. *To be published.*

[7] Eichten et al. Supercollider physics. *Rev.Mod.Phys.*, 56:589, 1984.

[8] M.Arneodo et al. Measurement of the proton and the deuteron structure functions, F_2^p and F_2^d. *Phys. Lett.*, B364:107, 1995.

[9] L.W. Whitlow et al. *Phys. Lett.*, B250:193, 1990.

[10] A.Bruel. Private communications.

[11] M.Dueren. The HERMES experiment: From the Design to the First Results. *Internal report DESY HERMES*, 95-02:129, 1995.

[12] A.Terkulov. Private communications. 1996.

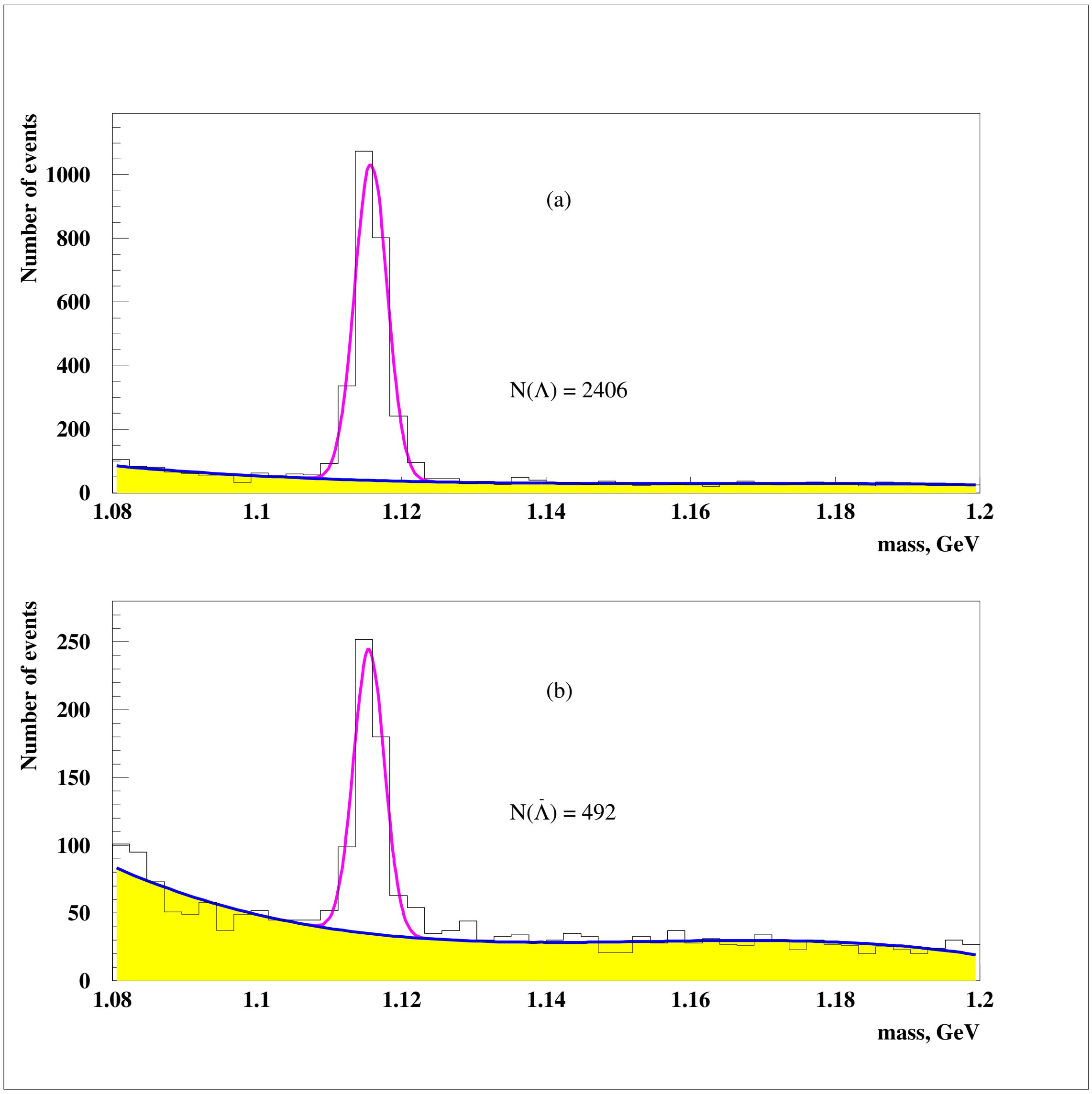

Figure 1: Invariant mass distributions for Λ (a) and $\bar{\Lambda}$(b) events with cuts.

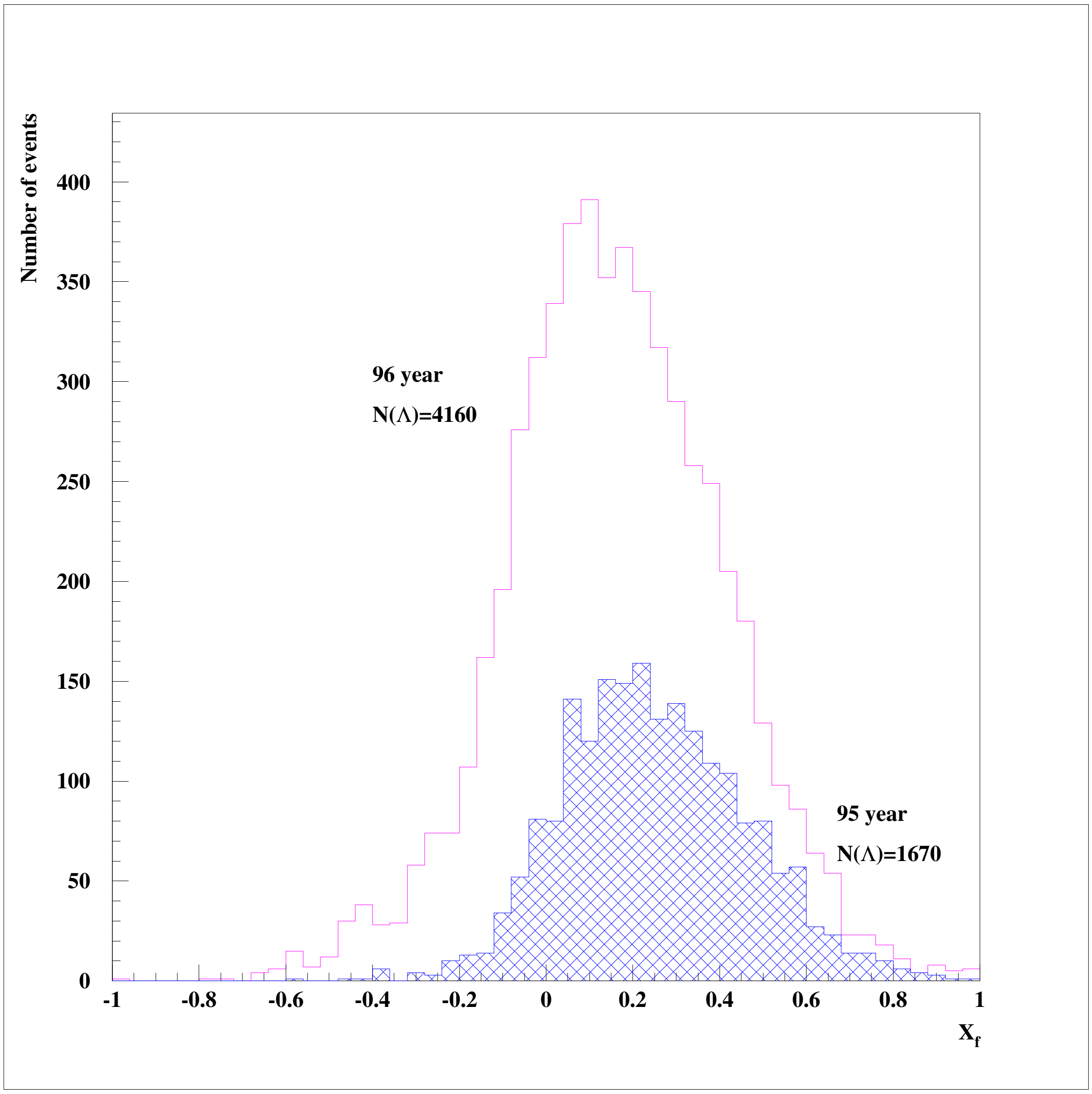

Figure 2: x_F-distributions for Λ-s obtained from 1995 and 1996 year data sets.

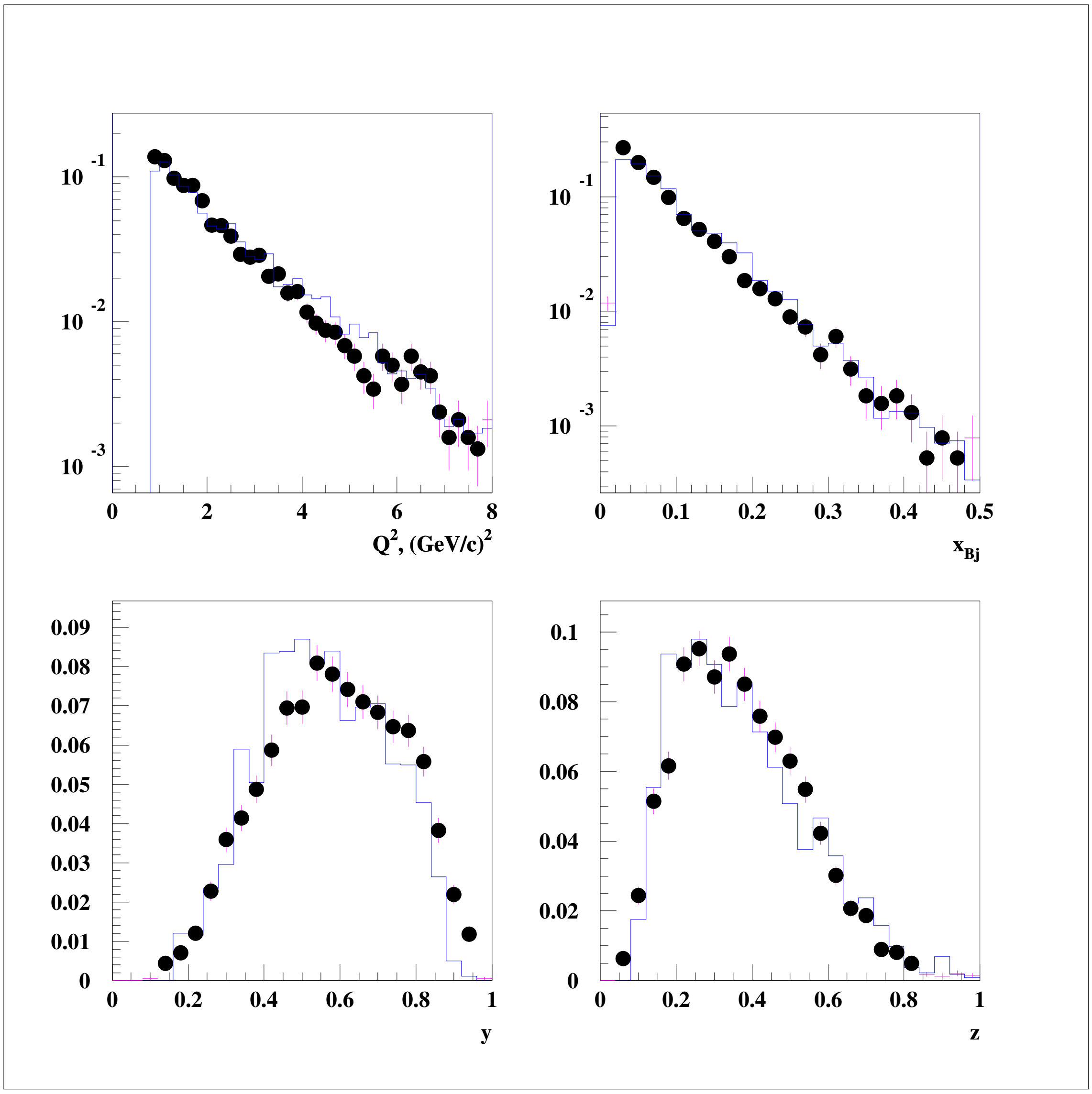

Figure 3: Normalized to unity experimental kinematic distributions(points) and HMC calculations (histograms).

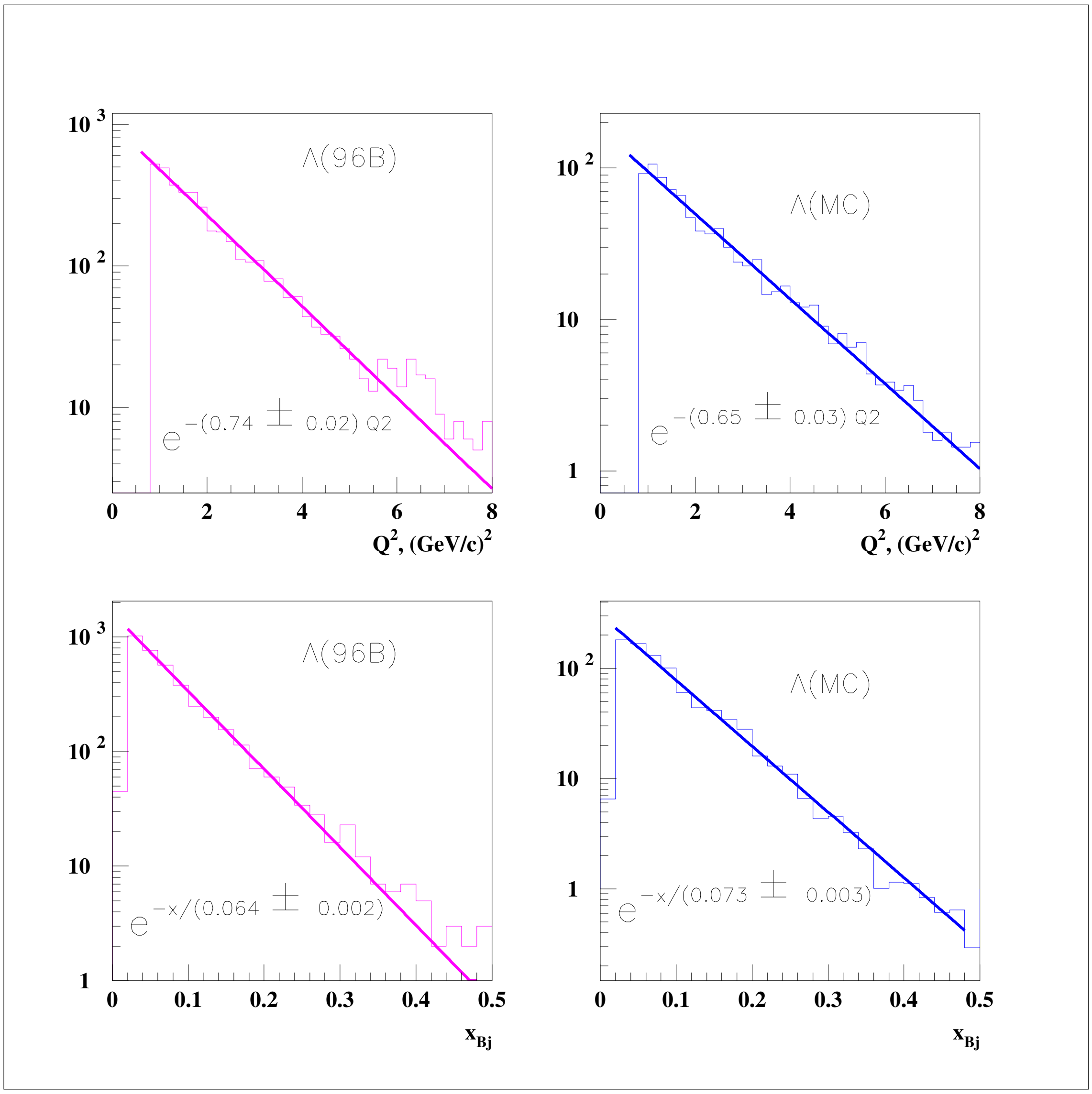

Figure 4: Slope parameters for Q^2 and x_{Bj} distributions,HMC and 1996 year data set comparison.

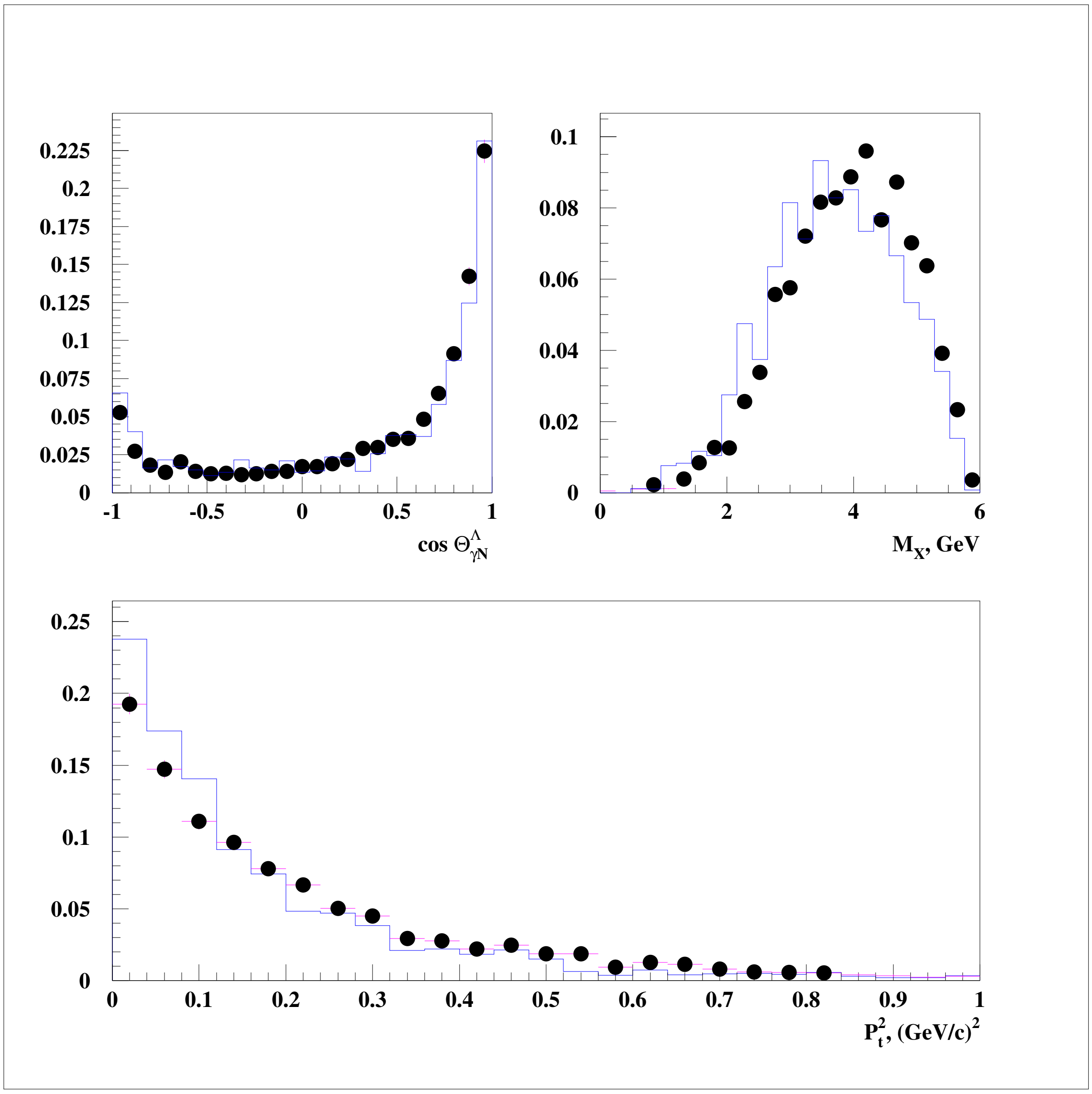

Figure 5: Normalized to unity experimental distributions(points) and HMC calculations(histograms).

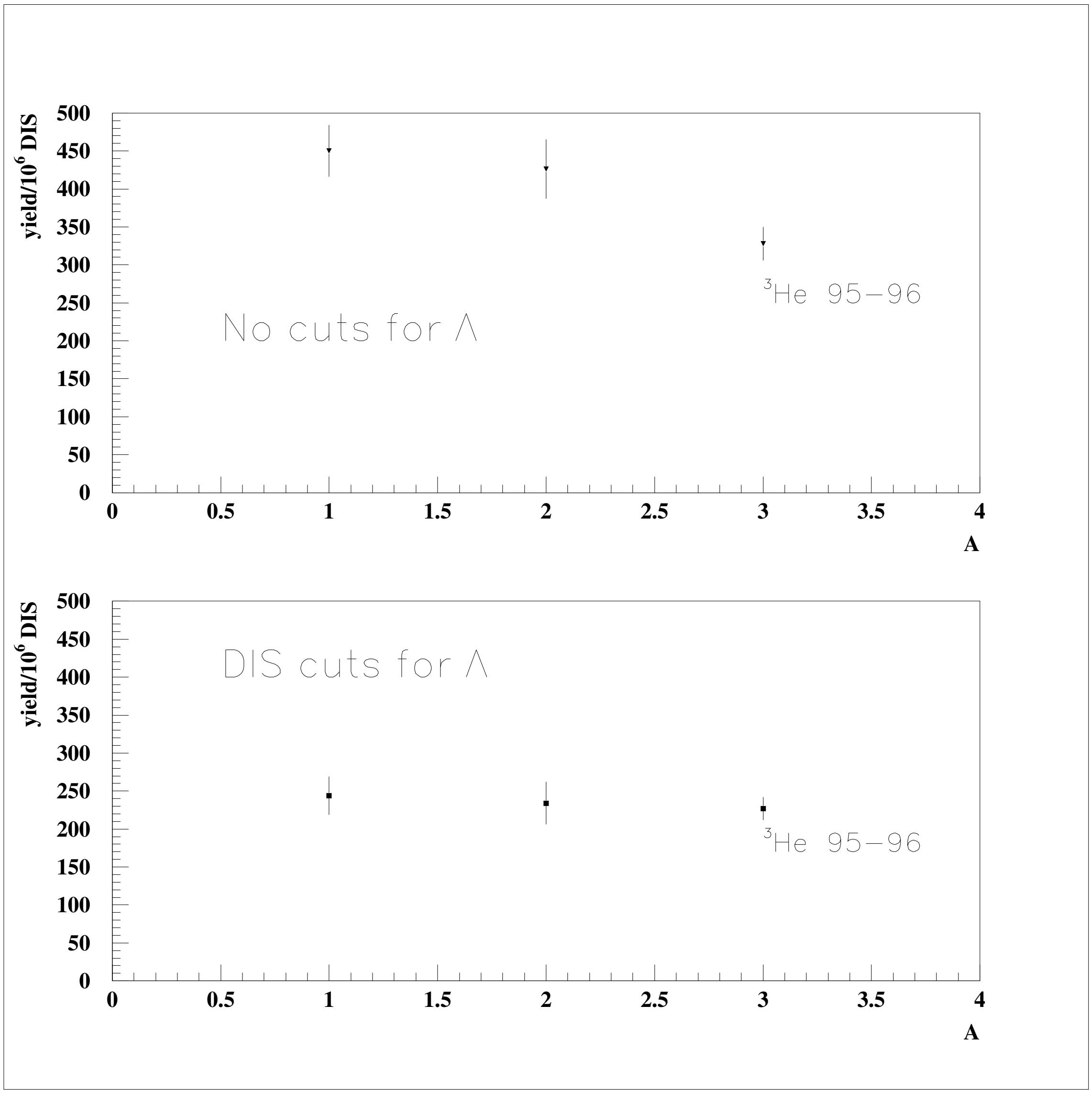

Figure 6: Λ yields normalized to 10^6 inclusive DIS events for hydrogen, deuterium and ^{3}He targets without DIS cuts (upper panel) and with DIS cuts (lower panel).

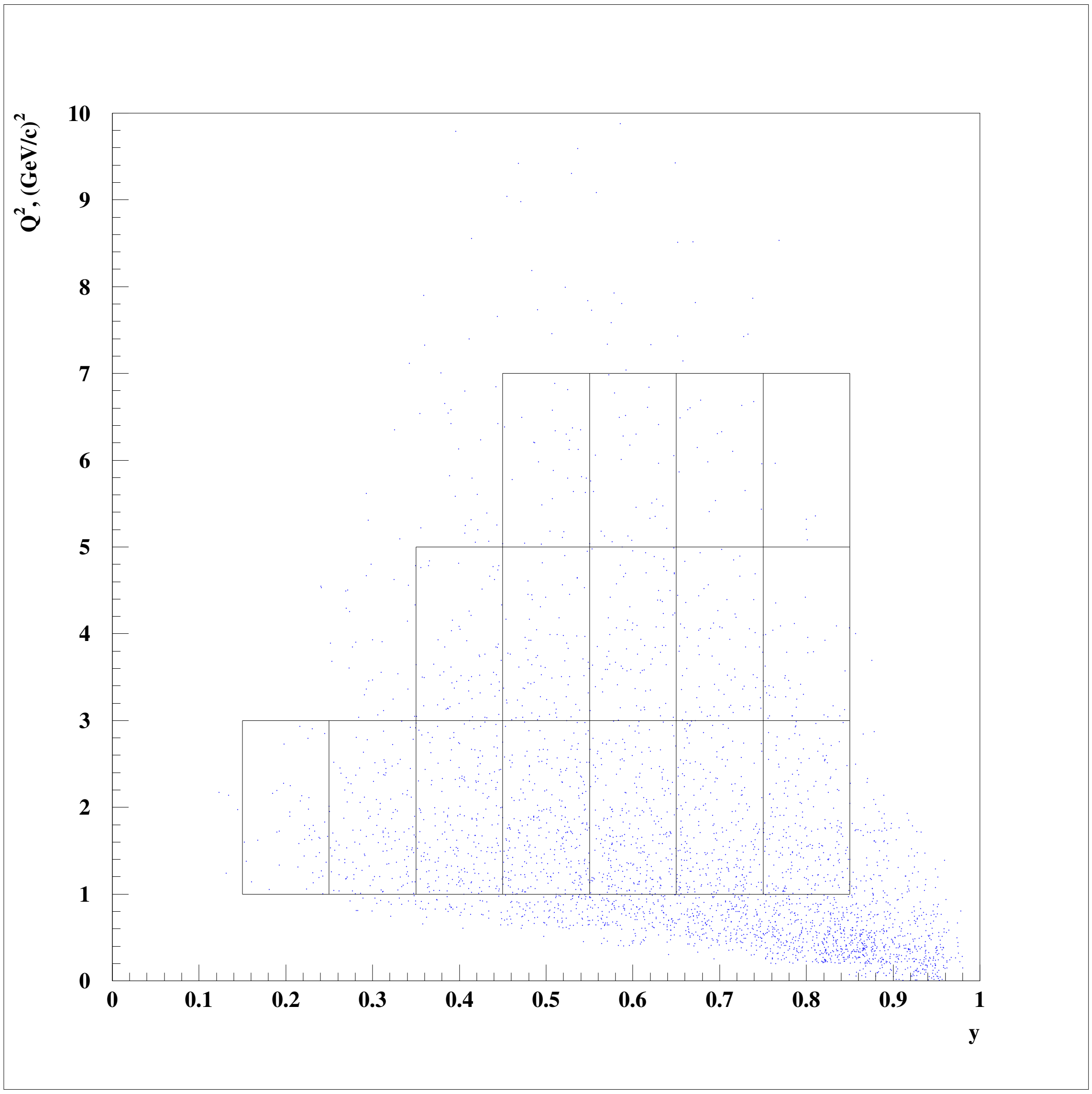

Figure 7: Q^2 versus y distribution of Λ events. The cells are shown in which HERMES detection efficiencies have been calculated.

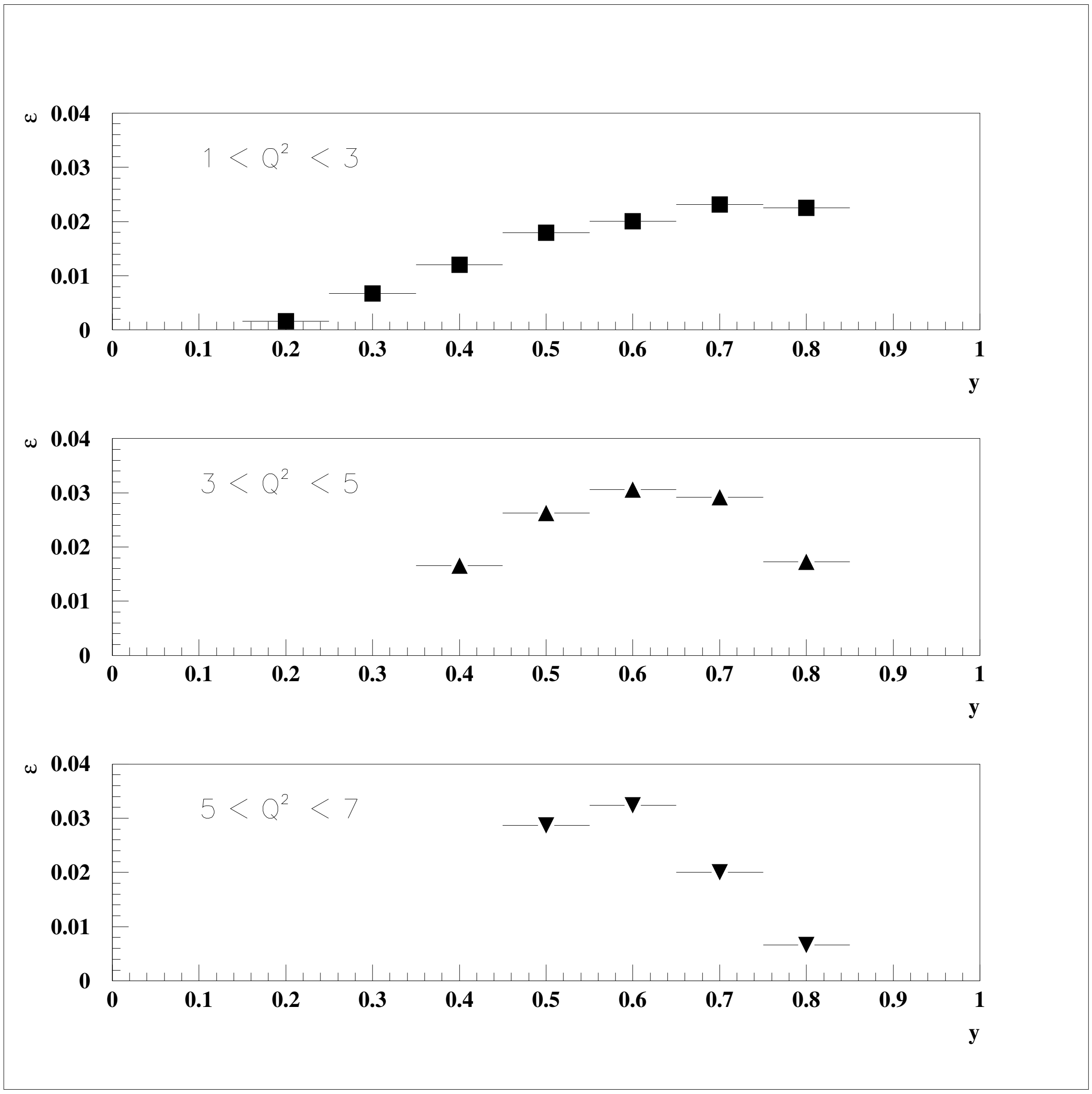

Figure 8: The HERMES detection efficiencies for Λ events.

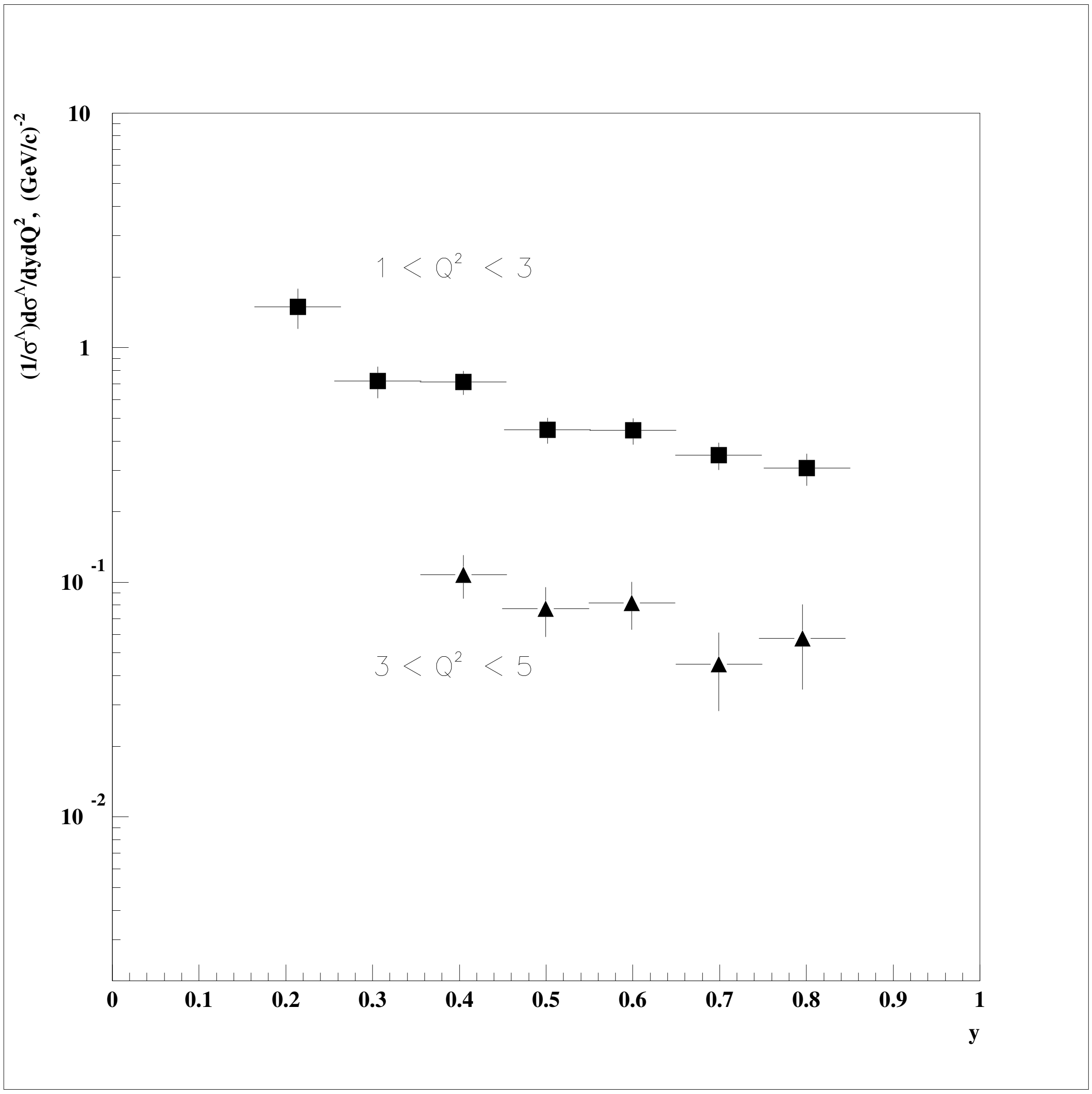

Figure 9: Normalized to unity cross sections of Λ electroproduction.

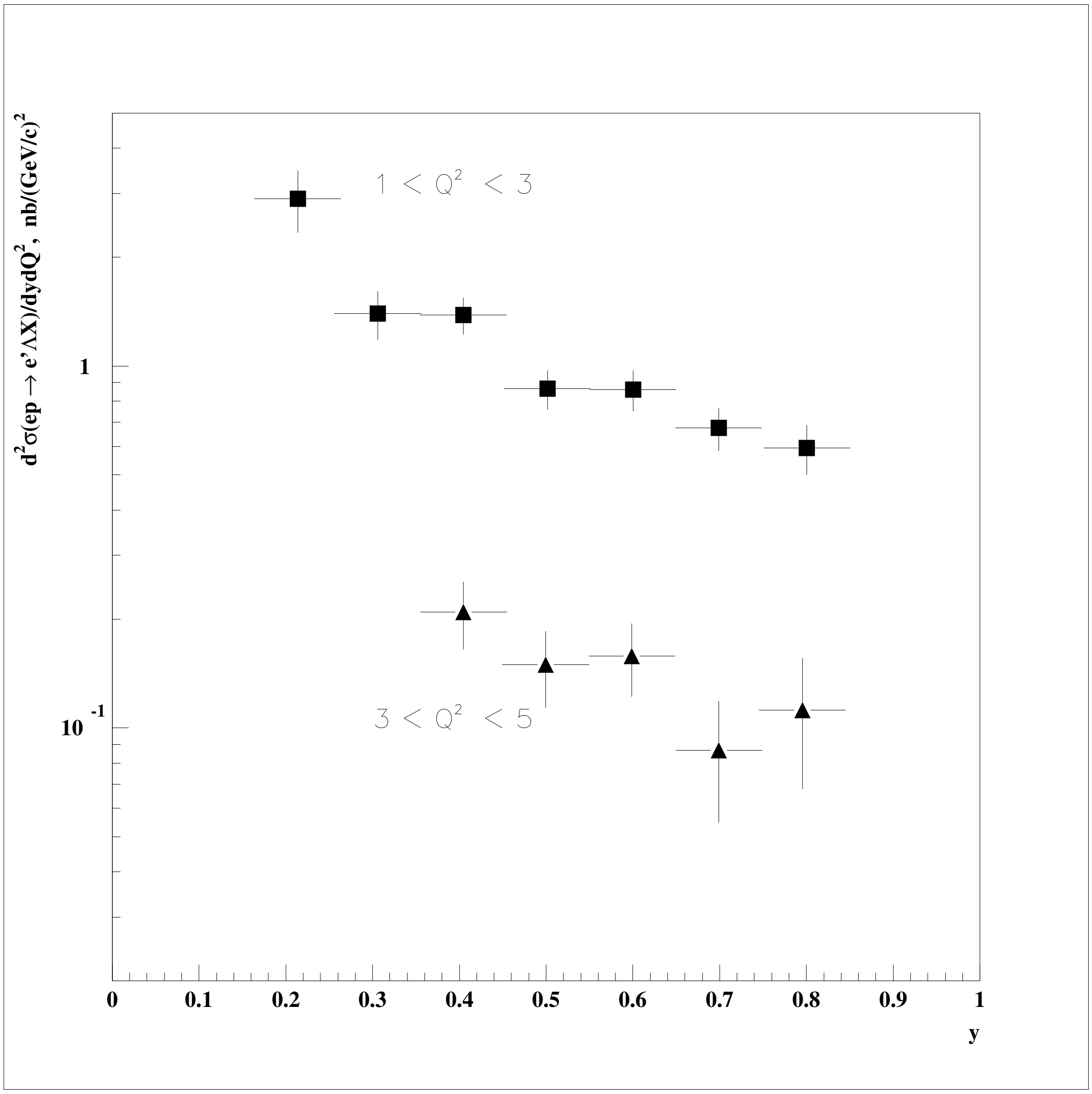

Figure 10: Absolutely normalized cross sections of Λ electroproduction.

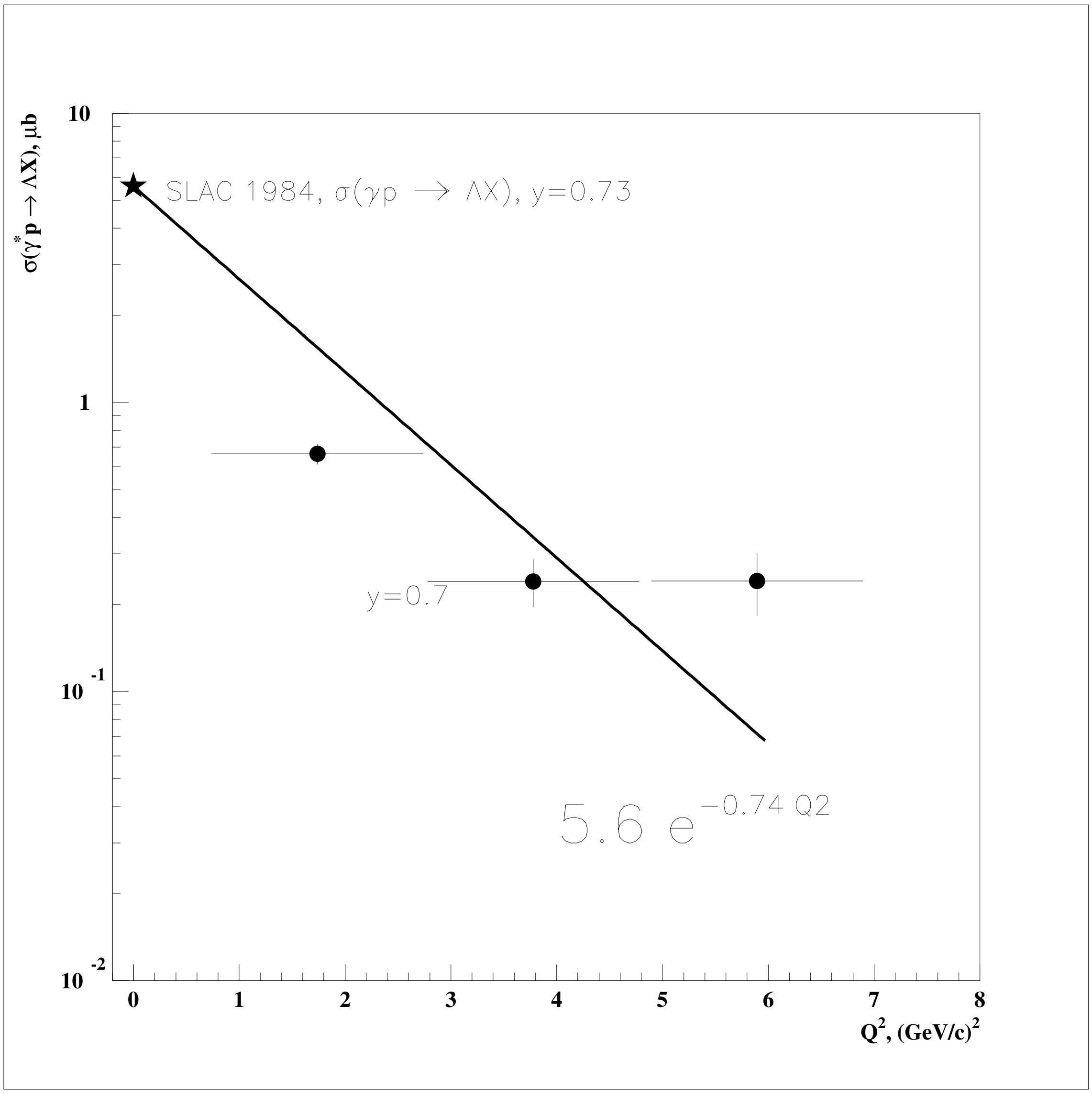

Figure 11: The total cross section $\sigma(\gamma^* p \to \Lambda X)$ in μb as function of Q^2 averaged at $0.55 < y < 0.85$

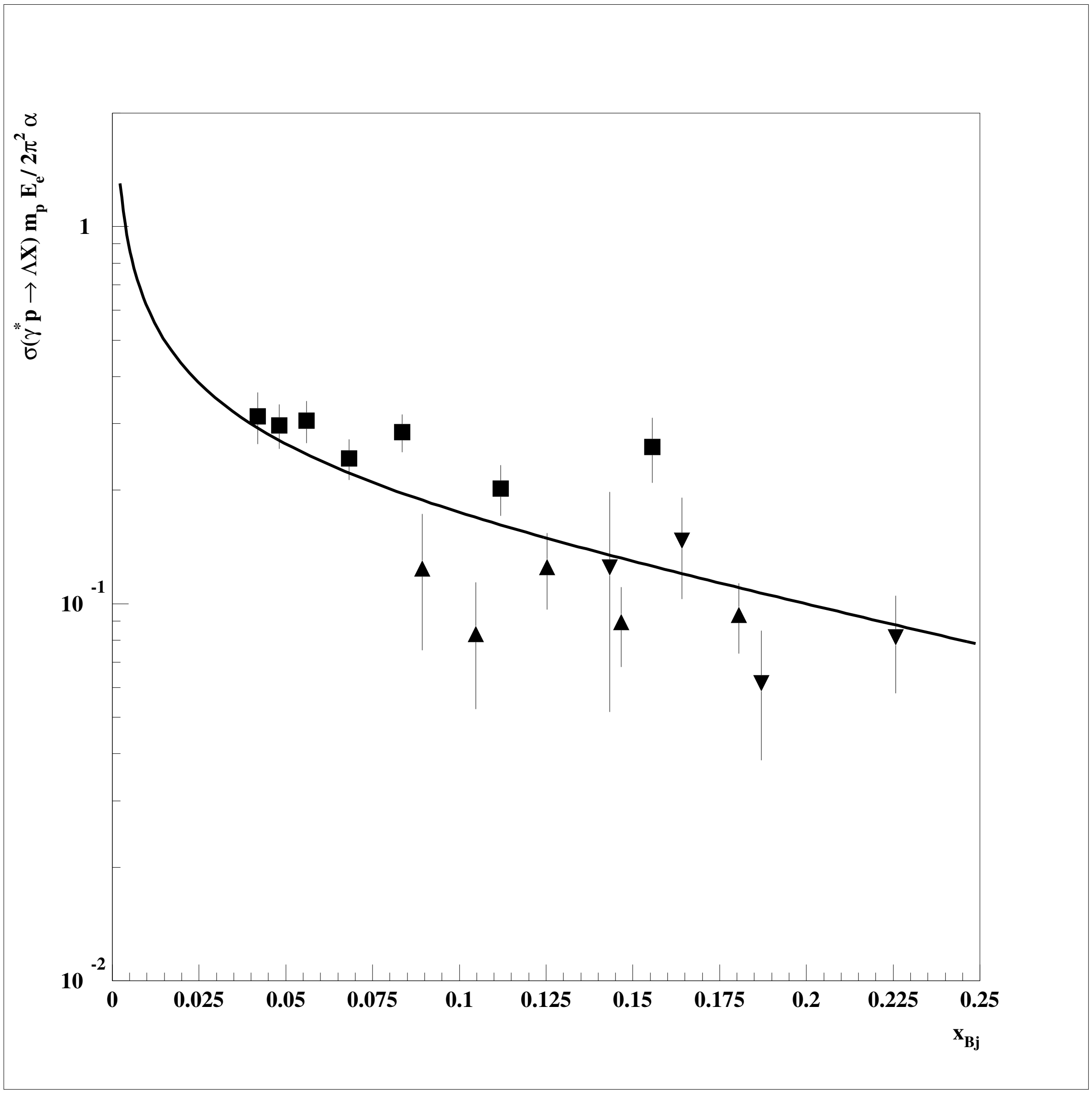

Figure 12: Comparison to QPM. Curve is $0.078 \cdot \frac{4}{9} u(x)$

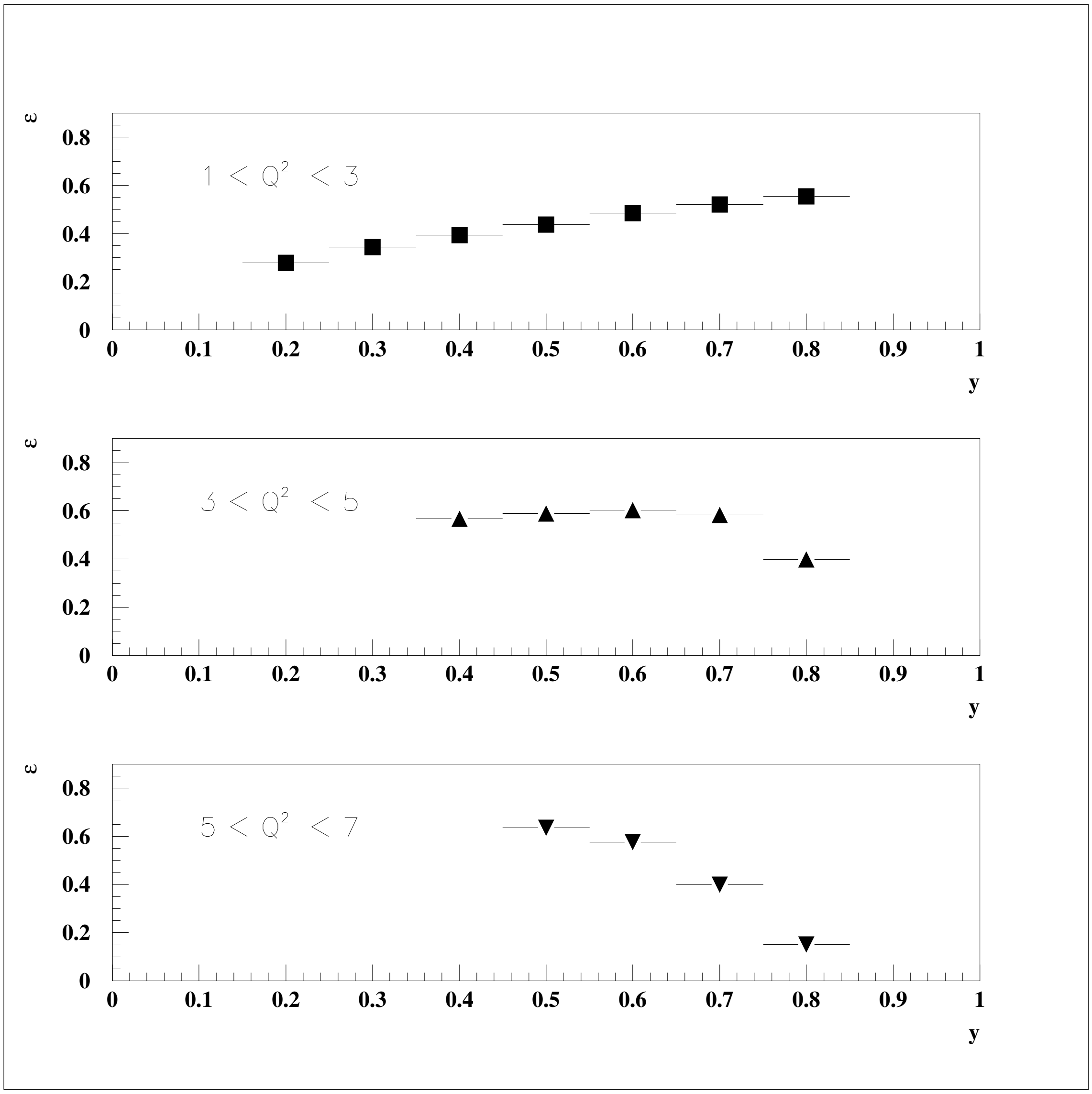

Figure 13: The HERMES detection efficiencies for inclusive DIS events.

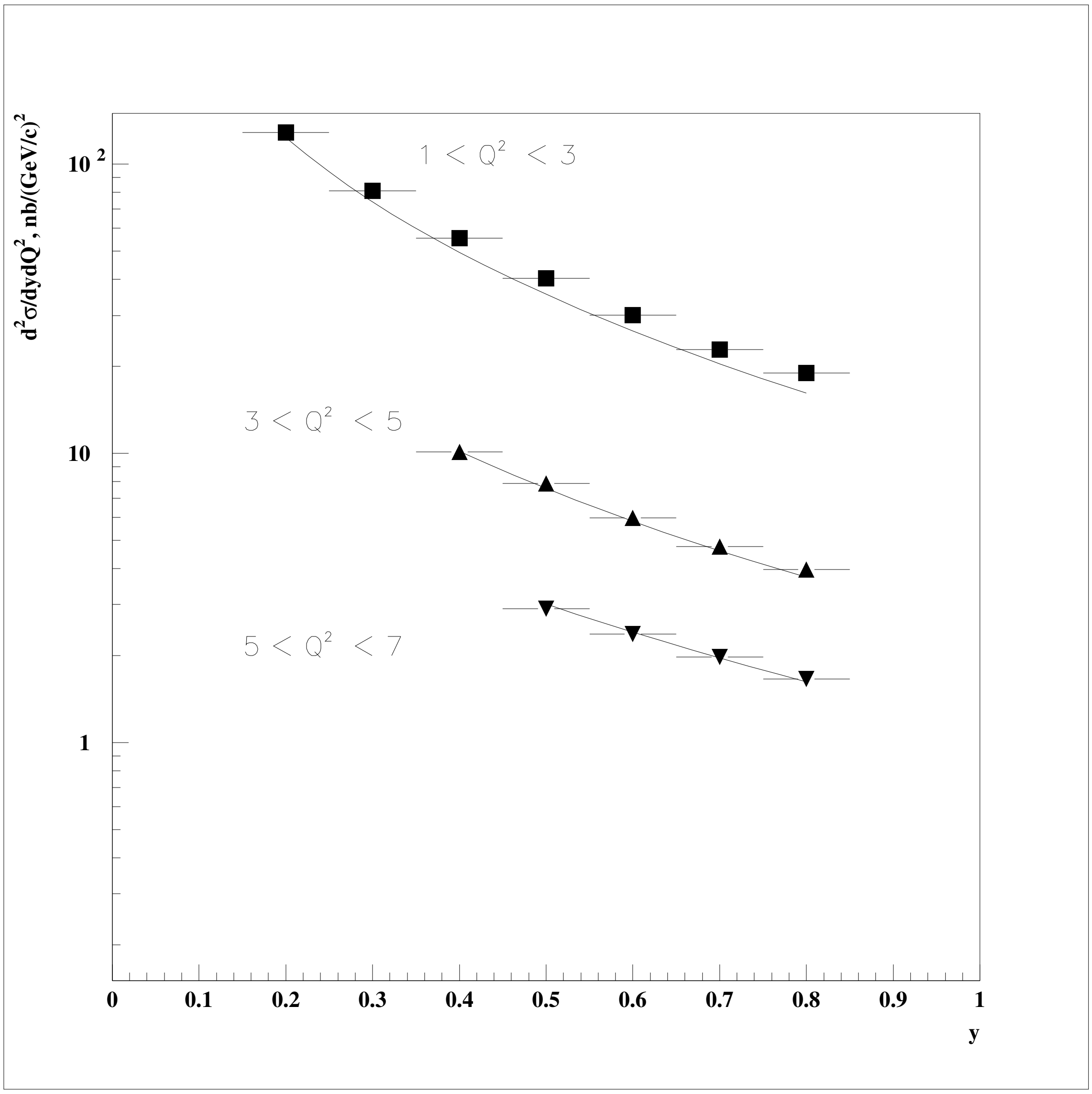

Figure 14: Absolutely normalized inclusive DIS cross sections $\frac{d^2\sigma(ep\to e'X)}{dydQ^2}$ with radiative corrections being included. Curves are calculated using the world data fit.